Measurements of Dynamo Activity and Spots of Zero-Age Main-Sequence Stars with TESS

Mai Yamashita[1] **[yamashita@nhao.jp]**, Yoichi Itoh[1], Yuhei Takagi[2], Yumiko Oasa[3]

[1]University of Hyogo (Japan), [2]National Astronomical Observatory of Japan, [3]Saitama University

We discuss the dynamo activities of zero-age main-sequence stars (ZAMSs) with their periodic light variation caused by a starspot and with the strength of the chromospheric emission lines. The amplitudes of the light curves of 33 ZAMSs in IC 2391 and IC 2602 were measured with *TESS* photometric data. The light curves can be grouped into the following four categories; single frequency, double-dipped, beater, and complex variability. The amplitudes of the light curves are $0.001 - 0.145\,\mathrm{mag}$, which are similar to those of ZAMSs in Pleiades (Rebull et al. 2016, AJ, 152, 133). The starspot coverages are $0.1 - 17\%$. It is known that the solar-type superflare stars with the large amplitude of the light curve have strong Ca II IRT emission line (Notsu et al. 2015, PASJ, 67, 33). We found that the light variations and $R'_{\lambda 8542}$ of the ZAMSs are as large as those of the most active superflare stars and two orders larger than those of the Sun. It is suggested that the high magnetic activity similar to that of the Sun continues from $30\,\mathrm{Myr}$ old. ZAMSs with single frequency in the light curve tend to have both large light variation, indicating large spot coverage, and saturated $R'_{\lambda 8542}$. ZAMSs with complex variability have small spot coverage ($\lesssim 1\%$) and small $R'_{\lambda 8542}$. We also detected 21 flares in the *TESS* light curves of 12 ZAMSs. The energy of the flares are estimated as $\sim 10^{33} - 10^{35}\,\mathrm{erg}$, which are comparable to the energy of superflare.

1-1. What happens in the chromosphere?

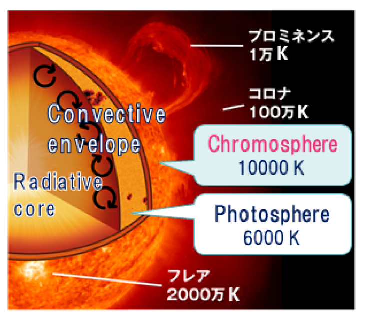

Fig. 1: Structure of a solar type star (ISAS/JAXA).

The temperature of the chromosphere gradually increases with radial distance to the photosphere. In an active chromospheric region, atoms emit permitted lines such as Hα and Ca II. It is claimed that chromospheric activity is driven by the magnetic field, which is generated by the dynamo process.

1-2. Starspot and chromospheric emission line

The chromospheric emission lines and the variation of the brightness caused by the starspot have been observed as the indicator of the activity.

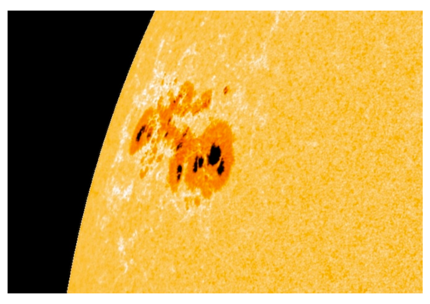

Fig. 2: Solar spots are often surrounded by emission regions, faculae (NASA/SDO)

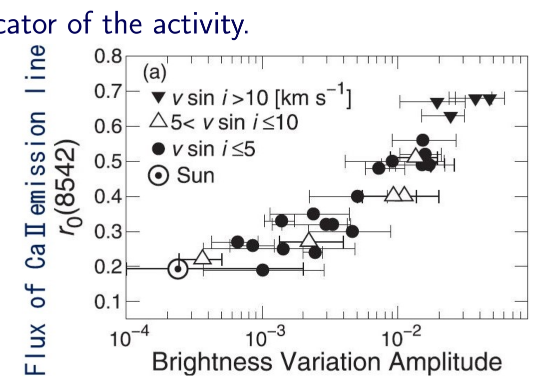

Fig. 3: The Ca II emission line ($\lambda 8542\,\text{Å}$) and the amplitude of the lightcurve of the superflare stars (Notsu et al., 2015)

- The largest solar spot have decreased the brightness by $\sim 0.1\%$.
- Solar-type main-sequence stars with the larger amplitude of the light curve (≒ larger spot) also show the brighter Ca II emission line (Fig. 3)

1-3. Dynamo activity of young solar-type stars

PMSs (CTTS・WTTS) and ZAMSs have

- faster rotation period, P (Fig. 4)
- slower convective turnover time (e.g. Landin et al. 2010)

than main-sequence stars.

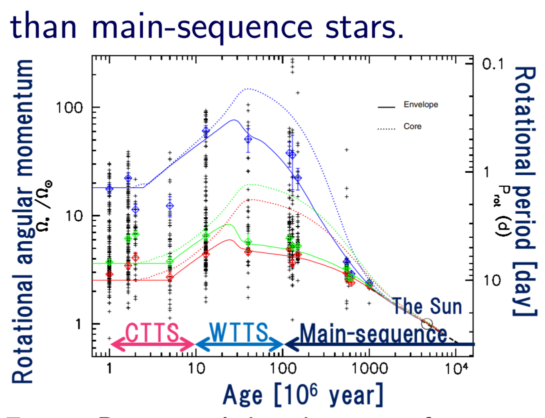

Fig. 4: Rotational distributions of solar-type stars (Gallet & Bouvier, 2013)

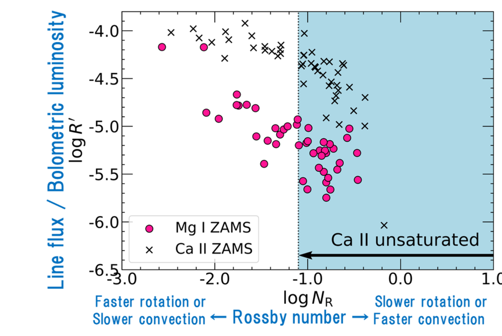

Fig. 5: Rotation-Activity Relation of infrared Mg I emission line ($\lambda 8807\,\text{Å}$) (Yamashita & Itoh, 2022a)

It is expected that PMS stars have active chromosphere because of their small Rossby numbers $\left(\equiv \frac{\text{rotational period, } P}{\text{convective turnover time, } \tau_c}\right)$

- Ca II emission lines (Fig. 5, ×): constant R' in $N_R \lesssim 10^{-1}$ (saturation)
- Mg I emission lines (Fig. 5, ●): not being saturated

1-4. Challenges

Q. For young stars, how does the starspot coverage relate the strength of chromospheric emission lines?

- Some ZAMSs have larger spot coverage of $4 - 17\%$ (Allain et al., 1996)
- Recently the light curves of ZAMS in the Pleiades cluster ($130\,\mathrm{Myr}$) are obtained from *Kepler* data

2. Target objects

1. 26 YSOs
2. 121 solar-type ZAMSs
   - IC 2602 ($\sim 30\,\mathrm{Myr}$)
   - IC 2391 ($\sim 50\,\mathrm{Myr}$)
   - Pleiades ($\sim 130\,\mathrm{Myr}$)
3. solar-type superflare stars
4. the Sun

* The binaries have been removed.

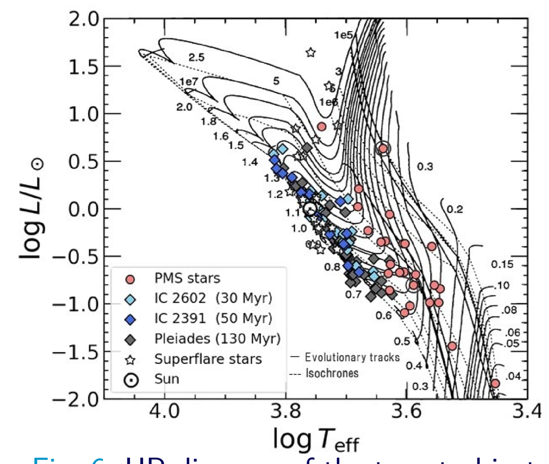

Fig. 6: HR diagram of the target objects

3-1. Result 1; Shape of light curves

We analyzed *TESS* photometric data with eleanor (Feinstein et al., 2019), and obtained the rotational period, P by conducting Lomb–Scargle periodogram analysis. We calculated the amplitudes of the light curves (10-90th flux).

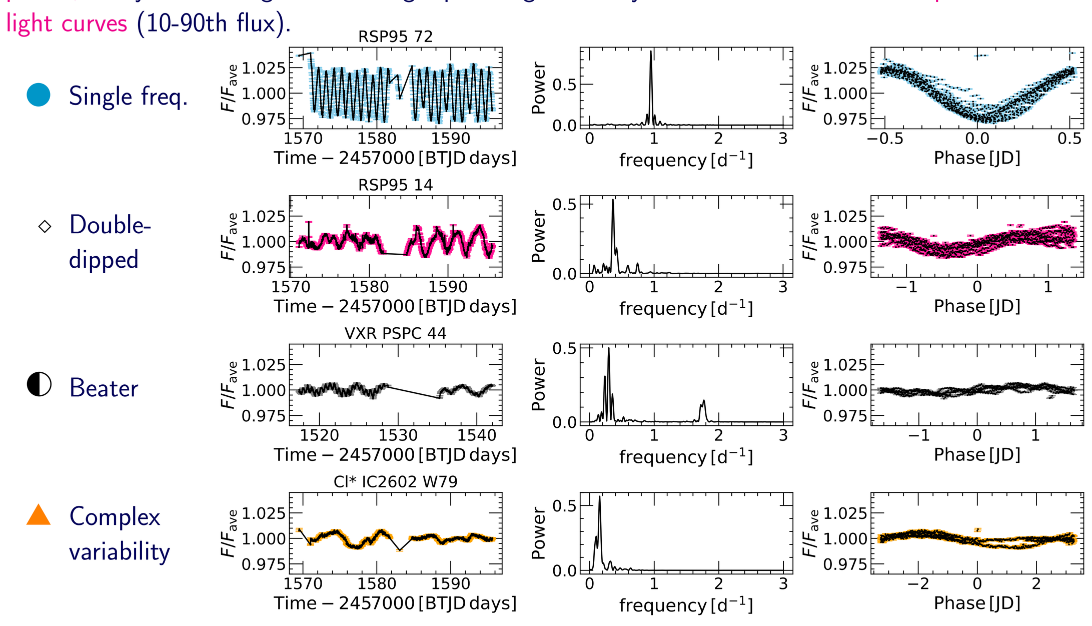

3-2. Amplitude vs Ca II emission line

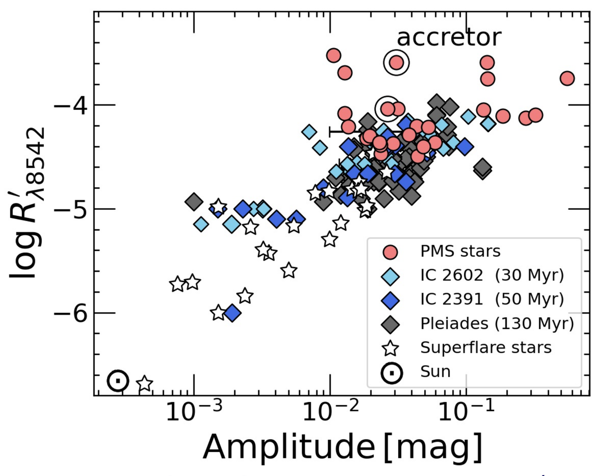

Fig. 7: The strength of the Ca II IRT emission line ($\lambda 8542\,\text{Å}$), $R'_{\lambda 8542}$ as a function of the amplitude of the lightcurve

- The objects with the larger amplitude of the light curve (≒ larger spot) also show the brighter Ca II emission line
- The ZAMS stars and PMS stars have about 2-3 orders
  - larger amplitude
  - larger R' (= brighter Ca II emission line)

  than the Sun and the superflare stars.
- The ZAMS stars are located on the extensions of the superflare stars.
- ZAMSs and PMSs could have enormous spot on their surface !
- The large-scale magnetic activity like the Sun may continues from the PMS stage.

3-3. Rotation-activity relation

X axis: Rossby number, $N_R \equiv \frac{\text{rotational period, } P}{\text{convective turnover time, } \tau_c} = \frac{2\pi R}{v \sin i}\frac{1}{\tau_c}$

Y axis: $R' \equiv \frac{\text{surface flux of the emission line, } F'}{\text{stellar total bolometric luminosity, } \sigma T_{\mathrm{eff}}^4}$

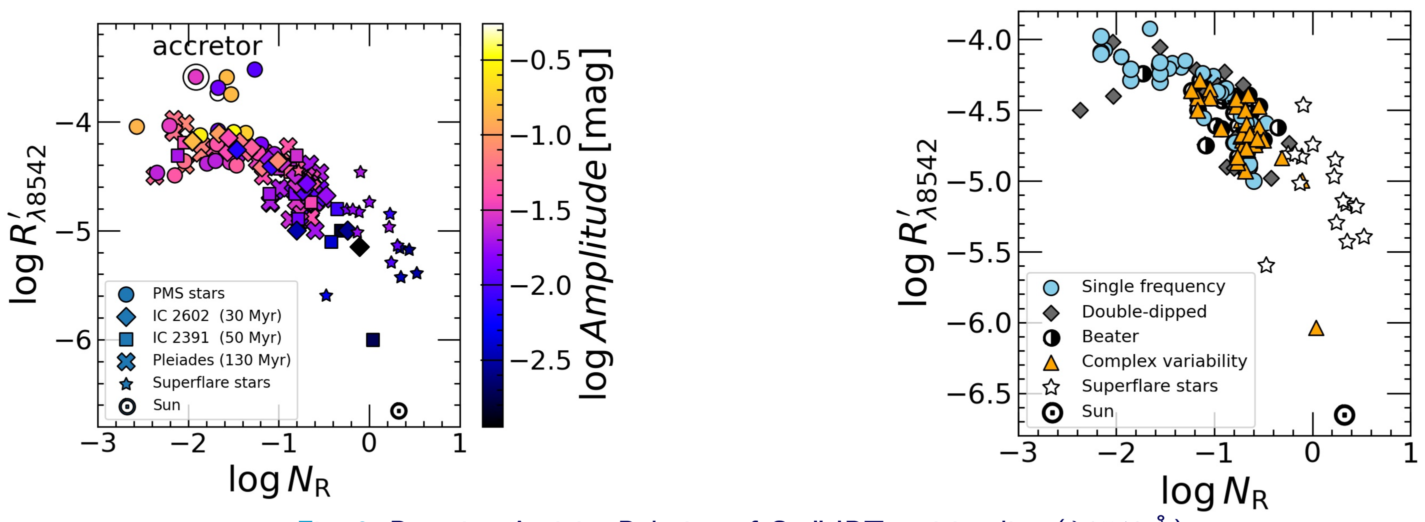

Fig. 8: Rotation-Activity Relation of Ca II IRT emission line ($\lambda 8542\,\text{Å}$)

- The objects with smaller N_R have
  - larger amplitude
  - larger R' (= brighter Ca II emission line)
- The objects with the larger chromospheric emission lines also have the larger spot / spot group.

A. ZAMSs with single frequency in the light curve (●) tend to have both large light variation, indicating large spot coverage, and saturated $R'_{\lambda 8542}$.

A. ZAMSs with complex variability (▲) have small spot coverage ($\lesssim 1\%$) and small $R'_{\lambda 8542}$.

Reference. R' of ZAMS: Stauffer et al. (1997), Marsden et al. (2009), the amplutude of lightcurve of ZAMSs in Pleiades: Rebull et al. (2016), F' and the amplitude of lightcurve of the solar-type stars: Notsu et al. (2015)

3-4. Period-color distribution and saturation

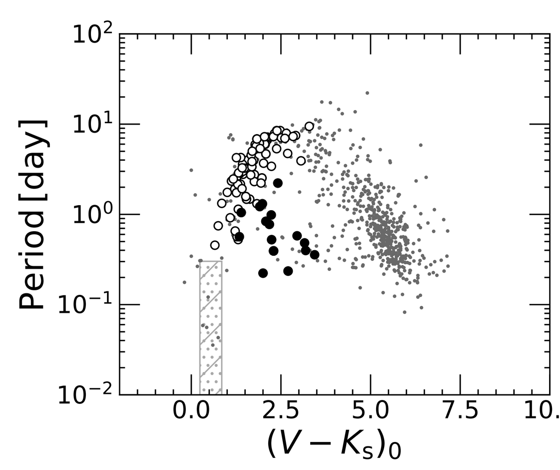

Fig. 9: Relationship between the $(V - K_s)_0$ color and the rotational period of ZAMS stars.

● The ZAMS stars in IC 2391, IC 2602, and Pleiades cluster whose Ca II emission lines are saturated tend to be distributed in the lower part of Fig. 9.

○ The ZAMS stars whose Ca II emission lines are unsaturated are located close to the majority of the Pleiades members.

It is suggested that the ZAMS stars whose Ca II emission lines are saturated have not reached the spin down stage yet.

4-1. Result 2; Flare detection

We detected sudden brightenings as flares (★ and ●).

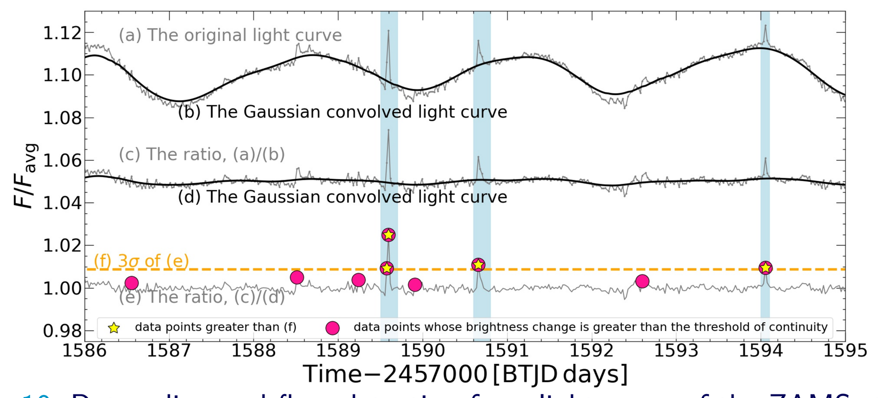

Fig. 10: Detrending and flare detection from light curve of the ZAMS star.

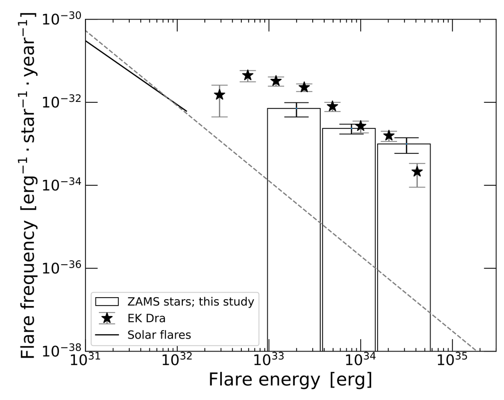

Fig. 11: Occurrence rate of flares on ZAMS stars and of solar flares

21 flares are detected in the light curves of 12 ZAMS stars in IC 2391 and IC 2602 ($1.5\,\mathrm{h} \lesssim$ duration time $\lesssim 15\,\mathrm{h}$).

4-2. Spot coverage vs Flare energy

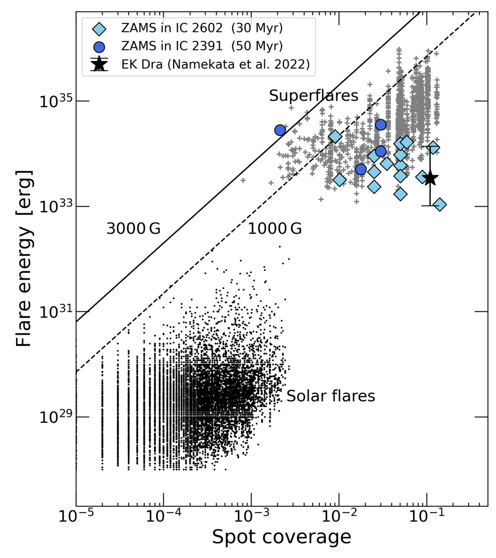

Fig. 12: Relationship between spot coverage, $A_{\mathrm{spot}}/A_{\frac{1}{2}\mathrm{star}}$, and flare energy, E_{flare}.

■ Spot coverage (The details are described in Notsu et al. 2019)

A spot area or flare-emitting area

$\frac{\Delta F}{F}$ normalized amplitude of light curve

$$A_{\mathrm{spot}} = \frac{\Delta F}{F} A_{\mathrm{star}} \left[1 - \left(\frac{T_{\mathrm{spot}}}{T_{\mathrm{eff}}}\right)^4\right]^{-1}, \quad (1)$$

$T_{\mathrm{eff}} - T_{\mathrm{spot}}$ is estimated with an empirical equation on T_{eff} (Berdyugina et al., 2005).

■ Flare energy E_{flare} (The details are described in Maehara et al. 2019)

$\frac{\Delta F}{F}$ the amplitude of a flare

$B(T, \lambda)$ the Plank function (assumed $T_{\mathrm{flare}} = 10000\,\mathrm{K}$)

$S(\lambda)$ the spectral response function of the *TESS* detector ($\lambda 6000 - 10000\,\text{Å}$; Ricker et al. 2015)

$$\frac{\Delta F}{F} = \frac{A_{\mathrm{flare}}}{A_{\frac{1}{2}\mathrm{star}}} \frac{\int B(T_{\mathrm{flare}}, \lambda) S(\lambda) d\lambda}{\int B(T_{\mathrm{eff}}, \lambda) S(\lambda) d\lambda}, \quad (2)$$

$$L_{\mathrm{flare}} = \sigma T_{\mathrm{flare}}^4 A_{\mathrm{flare}}, \quad (3)$$

$$\text{flare energy, } E_{\mathrm{flare}} = \int L_{\mathrm{flare}}(t) dt. \quad (4)$$

A. The energy, E_{flare}, is estimated to be $\sim 10^{33} - 10^{35}\,\mathrm{erg}$, which is comparable with the energy of a superflare.

4-3. Flare and saturation

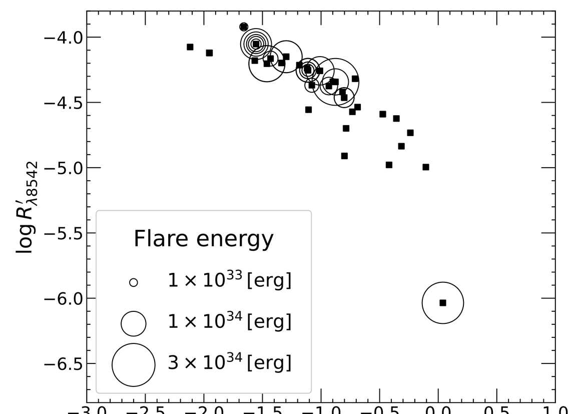

Fig. 13: The 21 flares are shown for the rotation-activity relationship of the ZAMS stars in IC 2391 and IC 2602.

- Most of the ZAMS stars in IC 2391 and IC 2602 on which the flares are detected are located in the saturated regime.
- Flares occur more frequently on the ZAMS stars having small N_R.
- Davenport (2016) show that GKM stars with small N_R show luminous flares.
- Medina et al. (2020) examined the relationship between N_R and the flare rate for mid- to late-M dwarfs. They found a high flare rate for small N_R stars.
- Our results indicate that small N_R objects experience superflares, even for ZAMS stars.

Allain, S., Fernandez, M., Martin, E. L., & Bouvier, J. 1996, A&A, 314, 173
Berdyugina, S. V. 2005, Living Rev Sol Phys, 2, 1
Davenport, J. R. A. 2016, ApJ, 829, 23
Feinstein, A. D., Montet, B. T., Foreman-Mackey, D., et al. 2019, PASP, 131
Gallet, F., & Bouvier, J. 2015, A&A, 577, 1
Landin, N. R., Mendes, L. T. S., & Vaz, L. P. R. 2010, A&A, 510, 1
Maehara, H., Notsu, Y., Namekata, K., et al. 2021, PASJ, 73, 44
Marsden, S. C., Carter, B. D., & Donati, J.-F. 2009, MNRAS, 399, 888
Medina, A. A., Winters, J. G., Irwin, J. M., & Charbonneau, D. 2020, ApJ, 905, 107
Namekata, K., Maehara, H., Honda, S., et al. 2022, ApJL, 926, L5
Notsu, Y., Honda, S., Maehara, H., et al. 2015, PASJ, 67, 33
Notsu, Y., Maehara, H., Honda, S., et al. 2019, ApJ, 876, 58
Noyes, R. W., Hamann, F. W., Baliunas, S. L., & Vaughan, A. H. 1984, AJ, 279, 763
Rebull, L. M., Stauffer, J. R., Bouvier, J., et al. 2016, AJ, 152, 113
Stauffer, J. R., Hartmann, L. W., Prosser, C. F., et al. 1997, ApJ, 479, 776
Yamashita, M., Itoh, Y., & Takagi, Y. 2020, PASJ, 72, 80
Yamashita, M., & Itoh, Y. 2022, PASJ, 74, 557
Yamashita, M., Itoh, Y. & Oasa, Y. 2022, PASJ, submitted

Conclusion: The high magnetic activity similar to that of the Sun continues from $30\,\mathrm{Myr}$ old.
The energy of the flares are estimated as $\sim 10^{33} - 10^{35}\,\mathrm{erg}$, which are comparable to the energy of superflare.